

# PIEZO MOTOR BASED HARDWARE TRIGGERED NANO FOCUS CAUSTIC ACQUISITION

L. B. C. Campoi\*, L. E. P. Vecina, G. S. R. Costa, G. B. Z. L. Moreno, N. L. Archilha  
Brazilian Synchrotron Light Laboratory (LNLS),  
Brazilian Center for Research in Energy and Materials (CNPEM),  
Zip Code 13083-100, Campinas, Sao Paulo, Brazil

## Abstract

MOGNO is a micro and nano X ray tomography beamline at Sirius. It was designed to operate with a cone beam, allowing for zoom tomography experiments via the use of a set of elliptical mirrors in a Kirkpatrick-Baez (KB) system. The main source produced by the KB system has  $120 \times 120 \text{ nm}^2$ , posing a challenge on the focus evaluation system, that has to probe such focus in a timely manner.

To tackle the KB system alignment evaluation, a diagnostic comprised of a stack of three linear inertia drive piezo stages and a fluorescence detector, acquiring data via hardware-triggered mesh scans was implemented. In the piezo stack, the stages are mounted along the X (horizontal, perpendicular to the beam path), Z (along the beam path) and YZ beamline directions. Moreover, a kinematic transformation was implemented due to the fact that a stage is placed at an angle and that the beam is not aligned with the sample stage stack. Mesh scans in the XZ and YZ can be divided in two parts: hardware triggered line scan acquisition along X or Y and software triggered steps along Z between scans. In this manner, the control is done via a collection of low-level controller macros and Python scripts, such that during the scans, the piezo controllers communicate with each other and the detector via digital pulses, orchestrated by the in-house TATU (Timing and Trigger Unit) software, reducing dead time between acquisition points.

The proposed system proved to be reliable to acquire beam profiles, providing caustics in both horizontal and vertical directions, and the acquired focus caustics indicate that the main source has a size of approximately  $416 \times 480 \text{ nm}^2$  at the moment.

## INTRODUCTION

Mogno is a micro and nano tomography beamline designed to provide users with high resolution, flexibility and high data throughput, via a cone-beam geometry with high flux. To achieve the desired resolution of 120 nm in each direction, the optical system is composed by three mirrors, a pair of elliptical multilayer mirrors in a KB (Kirkpatrick-Baez) system, that is also used to select the beam's energy (22 and 39 keV at the same time or 67.5 keV) [1], and a pre-KB elliptical mirror positioned as a horizontal focusing mirror (HFM) to compensate for inhomogeneities caused by the KB's HFM in the horizontal axis, as shown in Fig. 1. The mirrors have tight alignment budgets and at the first mirror

a nano focus is already produced in the horizontal, which poses challenges on how to evaluate such focus spot [2]. A similar problem occurs while tackling the KB's system alignment, however, the KB's focus must be evaluated in both horizontal and vertical planes, requiring a system with at least three degrees of freedom (DOF).

## EXPERIMENT DESCRIPTION

To evaluate the focus, a strategy based on the knife-edge method is proposed, where a sample is scanned across the beam and the fluorescence signal generated by the interaction of the X ray beam with the sample is collected in a fluorescence detector [2]. In the case of the KB's focus, the sample used is a calibration pattern from Applied Nanotools Inc. (ANT), which has Au features deposited on a Si substrate, and the detector used was a Hitachi Vortex ME-4 SDD, with a XSPRESS3 electronic from Quantum Detectors. For evaluation of the horizontal and vertical focus directions, L-shaped features with thickness of 600 nm and varying widths (1  $\mu\text{m}$ , 500 nm, 250 nm) were available.

Before each scan, the desired sample feature was positioned approximately on the beamline focus. The data acquisition was then composed by planar mesh scans, where fast line scans in a single direction perpendicular to the beam were executed, followed by single steps along Z. The subsequent scans were executed swapping the line scan endpoints, forming a snake motion. Data processing was done as described in [2]. The focus size is then acquired at different pitch angles of the KB mirrors, which can be compared to refine the beamline resolution.

## MECHANICAL ASSEMBLY

The diagnostic device assembly designed for the evaluation of Mogno KB's focus is an iteration on the assembly used during Mogno's pre-KB mirror alignment [2]. The assembly is composed by three linear piezo stages from Physik Instrument GmbH (PI) (QMotion series), which were selected based on the requirement of long range motion (millimeter scale), with precision in the nanometer scale. The stage set selected is composed by two stages with 13 mm of range (Q-545.140 QMotion) and one with 26 mm (Q-545.240 QMotion). The stage set was assembled (from bottom up) with the Q-545.240 positioned along the beamline's Z axis, a Q-545.140 positioned along the beamline's X axis and the second Q-545.140 was positioned at a 15° angle in the YZ plane. This assembly can be seen in Fig. 2, and it was chosen both to comply with the stages' mass load

\* lucca.campoi@lnls.br

Content from this work may be used under the terms of the CC BY 4.0 licence (© 2023). Any distribution of this work must maintain attribution to the author(s), title of the work, publisher, and DOI

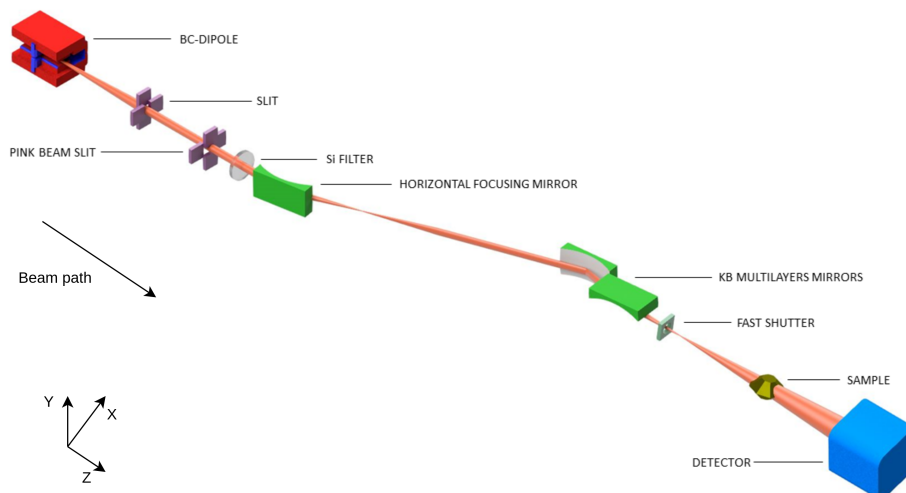


Figure 1: Mogno's optical layout.

restrictions (placing a stage in an orientation other than horizontal lessens its mass load capacity) and to improve the system's stability (avoiding the placement of a stage or the sample in an overhang condition).

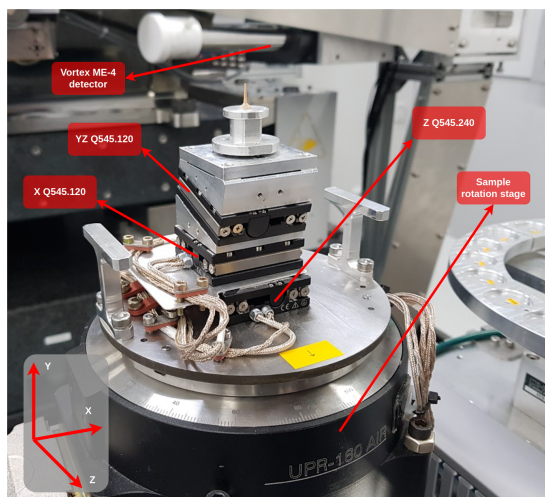


Figure 2: Stage stack assembly.

### Kinematics

With the designed assembly, the stage stack was placed on top of the beamline's rotational stage, giving a sample positioned 4 DOF when placed on top: X, Y, Z and  $R_Y$ . Due to the fact that the Y axis is not pure, the need for a kinematic transformation arises. In spite of the simplicity of the assembly, the 15° angle in which the Q-545.140 stage is positioned, restricts the range along Y to approximately 3.2 mm, moreover, it is needed to compensate the motion in the Z direction with the Q-545.240 stage, keeping the

sample motion purely along Y when the upper most stage is moving.

Furthermore, the beam is not aligned with the Z axis of the sample stage stack due to an deviation of 0.21° in  $R_X$  and 0.955° in  $R_Y$ , requiring a correction in Y and X axes while stepping in Z direction. These angles were determined analysing the full field image of a standard sample with an area detector. The procedure involved calculating the sample's center of mass displacement giving an well know step in Z, being possible to estimate the angular misalignment between the beam and the stage stack.

Finally, the designed system's kinematic matrix is as shown in Eq. (1), where  $\alpha$  represents mouting angle,  $\beta$  represents the beam misalignment angle in  $R_X$ ,  $\gamma$  represents the beam misalignment angle in  $R_Y$  and  $\phi$  represents the rotational stage current angle.

$$\begin{bmatrix} \cos(\gamma - \phi) & \sin(\gamma - \phi) \cos(\alpha) \cos(\beta) & -\sin(\gamma - \phi) \cos(\beta) \\ 0 & -\sin(\alpha) + \sin(\beta) \cos(\alpha) & -\sin(\beta) \\ -\sin(\gamma - \phi) & \cos(\alpha) \cos(\beta) \cos(\gamma - \phi) & -\cos(\beta) \cos(\gamma - \phi) \end{bmatrix} \quad (1)$$

### CONTROL ARCHITECTURE

For the required planar scan to be executed in a timely manner, a fly-scan approach was considered, however, the piezo stages use an inertia drive motion mechanism, meaning that, periodically, there is a decoupling between the actuator and the motion platform of the mechanism, that results in a momentarily following error. As shown in Fig. 3, the decoupling of the mechanism causes an error in the hundreds of nanometers scale. During the evaluation of the focus, the desired step size was 20 nm, which is an order of magnitude lower than the error intrinsic to the stage mechanism. If a fly-scan was implemented, the data points occurring during the mechanism's decoupling could be blurred due to the motion stage jumping around, meaning that data could be generated

out of order or repeatedly, as the stage comes back to its trajectory and passes through the desired points a second time. This fact made it necessary to implement a hardware-triggered step scan, in which the stage has time to settle and later to trigger the acquisition at each point.

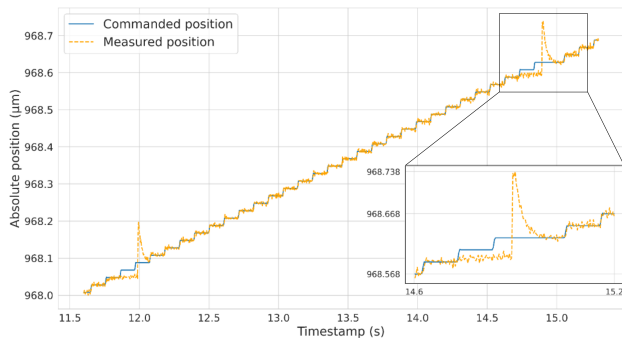


Figure 3: Section of 1D step-scan comparison between commanded and measured position, where the periodic position error spikes can be seen in detail.

The QMotion series stages used each have their own standalone controller, this means that for each plane that has to be scanned a set of controller macros was needed. Moreover, in the case of the YZ plane scan, communication between controllers was also implemented.

In general, each scan is composed by three different scopes: a high-level Python package used to configure scan variables and devices via EPICS, a set of controller macros that execute the fast movement loop, and hardware communication to trigger acquisition and subsequent steps. Figure. 4 shows the block diagram for a generic hardware-triggered step-scan implemented.

During the execution of the caustic profile acquisition, the user interacts with the high-level Python package via a Jupyter notebook. This package was developed using object orientation, so it is composed by a set of objects that abstract the scan procedure. 1D scans are encapsulated into a set of classes, moreover, 2D scans are composed by a set of 1D line scans, so their objects are dependent on 1D scan objects through composition. The interface defined for each scan object lets the user configure variables that are then passed to each device in use (motion stages, detector and trigger management system). In the case of 2D scans, the movement between 1D hardware-triggered scans is controlled via a set of EPICS IOCs, one for communication with each controller and another built on top of the individual stages' IOCs that controls the 3-axis piezo stack, taking into account the kinematic matrix Eq. (1). The kinematic IOC was built in Python using the PCAsPy package, and in addition to allowing for position control and feedback in the beamline's coordinate system, it also provides access to data gathered by the controller in the beamline's coordinate system and access to each underlying stages' variables. The controller macros are started via commands sent to through an Asyn-Record, allowing the Python scripts to probe the controller directly for scan control variables.

## Controller Macros

As shown in Fig. 4, the controller macros developed are composed by a configuration step followed the motion loop. During configuration, the controller's digital IO interface and data gatherer are configured. Moreover, the *counter* and *finished* loop control variables are zeroed prior to the movement of the stage to the scan's initial position, where a first digital signal is sent to the TATU [3] trigger interface. The acquisition loop is then executed, with the trigger interface signaling each next step after waiting for the detector to collect the fluorescence signal. At the end of the loop, when the *counter* control variable reaches the number of requested points, the *finished* variable is set to one and the stage's velocity and acceleration are reset to their default values.

The macro described was deployed as is to control each of the X stage during the XZ plane scan. However, for the YZ plane scan it was needed to deploy the macros to each controller in use and to configure the trigger interface to coordinate the steps for both YZ and Z stages. In this way, during the motion loop, motion is executed by the YZ stage, which triggers the Z correction that finally triggers the acquisition by the detector.

## RESULTS

### Control System Evaluation

To evaluate if the implemented scans are working correctly, the data gather functionality of the E-873.1AT controllers were used to collect the commanded and measured position of each motion stage, the motion and IO ports status during hardware-triggered scans. The controllers were configured to capture data at a frequency based on the total 1D scan period, as the controllers only support the acquisition of 7616 data points at a time. During these tests, the step amplitude on the beamline's X and Y axis was set to 20 nm, the slow Z axis step used was 20  $\mu\text{m}$ , the acquisition time was set to 200 ms, and the velocity and acceleration for each stage was set to 1 mm and 1 mm/s<sup>2</sup>, respectively.

The on target state was used to determine the positions in which the acquisitions should take place. The mask produced by the on target state was used to separate the plateaus related to exposure positions in the commanded and measured position arrays, which were compared to generate a following error array.

Using the position error data, the mean error during acquisition was estimated and the error distribution for each stage is shown in Fig. 5. The distributions show that during acquisition of a data point, the stage stack remains static within a window less than the step size, with the mean error of  $4 \pm 3$  nm for X,  $2 \pm 1$  nm for YZ and  $8 \pm 7$  nm for Z.

In addition, using the commanded position within acquisition points, it was possible to calculate the mean acquisition position, from which the actual executed step size could be estimated for each stage in both the scan planes. The step size in YZ scans for each motion stage was obtained

Content from this work may be used under the terms of the CC BY 4.0 licence (© 2023). Any distribution of this work must maintain attribution to the author(s), title of the work, publisher, and DOI

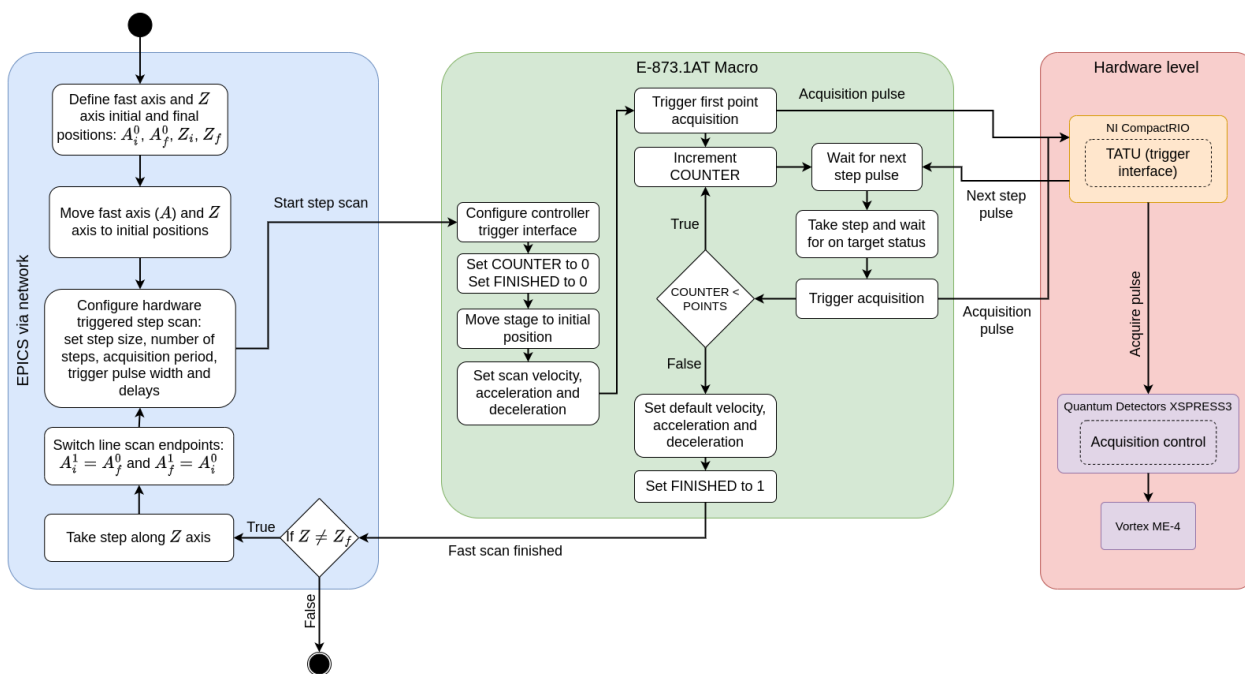


Figure 4: Block diagram for caustic scan, where A represents the axis where the hardware-triggered step-scan takes place.

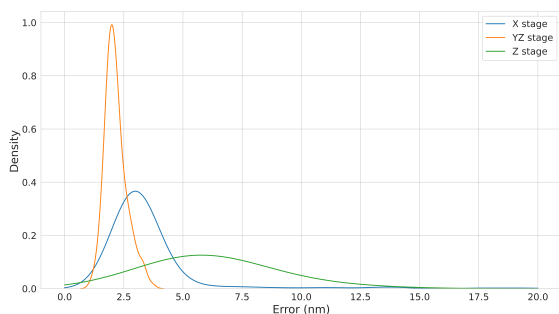


Figure 5: Mean error density distribution during acquisition plateaus.

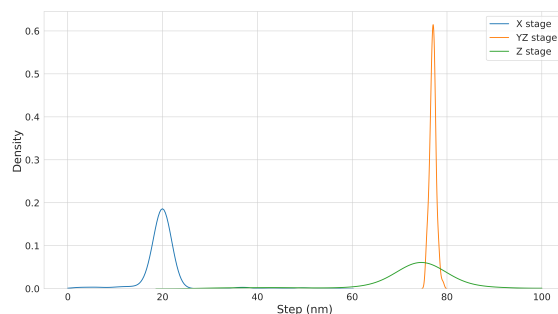


Figure 6: Mean step amplitude density distribution.

applying the inverse kinematic matrix obtained from Eq. (1), considering the 20 nm requested step size, resulting in steps of 77 nm for the YZ stage and 75 nm for the Z stage. The resulting step amplitude distributions are shown in Fig. 6, and the mean step sizes observed were  $20 \pm 5$  nm for X,  $77 \pm 1$  nm for YZ and  $75 \pm 13$  nm for Z. Due the fact that the plateaus analyzed do not contain the periodic position error, the normal-like distributions observed are expected, as only the random position variation is being measured.

Figures 5 and 6 which it can be seen that the stages positioned farther up along the stack are more stable, with the standard deviation of the YZ stage being lower than 1 nm, while the Z stage has a standard deviation in the tens of nanometers scale. This difference in stability can be attributed to the fact that, being at the base and carrying its most mass, the Z stage can be excited by vibrations while its load moves around (motion from X and YZ stages), which

is more pronounced in the case when the YZ stage is actuated, as it actuates along the same direction as the Z stage.

Furthermore, during the analysis of the position error within acquisition and the step amplitude, some limitations were observed. The fixed number of data points provided by the controller's data gather solution meant that, for the acquisition of data for a whole 1D scan the frequency of acquisition had to be lowered, leading to more noisy trajectory profiles. In addition, the fact that discontinuities were observed during the motion mechanism decoupling made it necessary to filter out these points when trying to identify acquisition plateaus in the trajectory. These facts led to some acquisition plateaus being described by only a few point, which could lead to outliers in the error and step amplitude distributions. Finally, the stages performance within the scan context was only evaluated considering the actuating direction, so no transversal motion was analyzed.

The scan execution time was also analyzed. During a 1D scan, the dead time is composed by the sum of the step

motion period, however during a 2D scan, the motion along Z, beamline state data gathering, IO operations and software triggered motion period also have to be considered.

For X axis 1D scans, the mean step period measured is 25 ms, leading to a dead time of approximately 12.5%. However, analysing whole 2D XZ scans, the mean dead time is estimated at approximately 23%. For Y axis 1D scans, YZ and Z motion are sequential, meaning that the step period is composed by the the sum of both stages' steps, leading to a estimated mean step period of 41 ms and a dead time of 21%. In the case of whole 2D YZ scans, the estimated dead time was of 35%.

### KB Alignment Evaluation

With the selected Au sample, it was possible to acquire caustics only in the lower beamline energies (22 and 39 keV), as in the 67.5 keV beamline configuration, the interaction between the beam and the sample produces a weak signal, making it difficult to align the sample and also leading to noisy data.

Although the mirrors' alignment is still being refined, preliminary results using an exposure time of 200 ms were obtained. Figure 7 shows the gradient along the axis perpendicular to the beam for caustics acquired on the XZ and YZ planes.

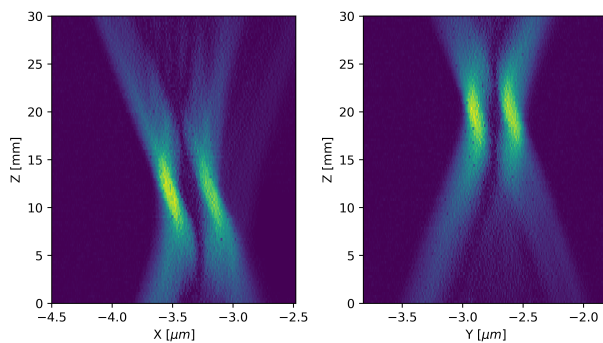


Figure 7: Gradient of caustic along the direction perpendicular to the beam path, for XZ (left) and YZ (right) scans with 100  $\mu\text{m}$  steps along Z and 20 nm steps along the perpendicular direction and 200 ms of exposure.

From the gradient of the caustics in Fig. 7, the focus size in each plane was estimated via the FWHM of the peaks seen in the smallest cross-section, leading to a estimated focus size of 416 nm in the X direction and 480 nm in the Y direction. Although the focus size still needs to be refined, it has not limited the continued commissioning of other beamline systems and capabilities, such as zoom tomography, considering the obtained focus size as the maximum resolution limit for 2D images acquired at the beamline.

### CONCLUSION

Via the use of linear piezo stages, it was possible to implement a set of scan procedures that enables the acquisition

of beam caustics at Mogno KB's focus. The resulting experimental setup is composed by hardware-triggered step-scans followed by software-triggered steps along the beam direction, due to intrinsic errors caused by the stages' mechanisms. The hardware-triggered scans were implemented with the help of controller macros and represent a solution to capture caustics in a period that can still be improved, as the scans' dead time can reach up to 35% of the elapsed scan time.

Moreover, via the analysis of the trajectories executed during scans, it was shown that the designed assembly and control solutions made it possible to execute the desired step amplitude of 20 nm in each direction and to keep the sample still during acquisition plateaus. In addition, it was noted that the stability of the stages in the stack is not homogeneous, as the topmost stage is the most stable, while the bottom stage shows the largest instability.

Finally, using the proposed method, the focus size was already refined to a condition that does not limit the commissioning of other beamline systems, as the achieved focus size of 416 nm in the X direction and 480 nm in the Y direction is smaller than the current tomographic resolution limit. In spite of that, the focus refinement is still ongoing, although it has been difficult to achieve smaller focus sizes while also removing effects such as astigmatism with only the analysis of the caustics. Currently, the caustic analysis is being coupled with the analysis of 2D images captured with area detectors. In addition, improvements to the scans' dead time in the future should be prioritized, as it would allow for more iterations of the mirrors' positions.

### ACKNOWLEDGEMENTS

The authors thank Mogno group and all the LNLS technical support groups for the valuable discussions and great support in the assembly and commissioning of the beamline, specially the control, software, projects and optics groups. The authors also thank Equinor Brazil. This work is supported by the Brazilian Center for Research in Energy and Materials (CNPEM), under the supervision of the Ministry of Science, Technology, and Innovation (MCTI).

### REFERENCES

- [1] N. L. Archilha *et al.*, "MOGNO, the nano and microtomography beamline at Sirius, the Brazilian synchrotron light source", *J. Phys.: Conf. Ser.*, vol. 2380, p. 012123, 2022. doi:10.1088/1742-6596/2380/1/012123
- [2] L. B. C. Campoi *et al.*, "Elliptical mirror position correction based on caustic analysis", *J. Phys.: Conf. Ser.*, vol. 2380, p. 012089, 2022. doi:10.1088/1742-6596/2380/1/012089
- [3] J. R. Piton *et al.*, "TATU: A Flexible FPGA-Based Trigger and Timer Unit Created on CompactRIO for the First Sirius Beamlines", in *Proc. ICALEPCS'21*, Shanghai, China, Oct. 2021, pp. 908-911. doi:10.18429/JACoW-ICALEPCS2021-THPV021